

# Merging Two Functions in a Single Rh Catalyst System: Bimodular Conjugate for Light-Induced Oxidative Coupling

Jinwoo Kim, Dongwook Kim, and Sukbok Chang\*

Cite This: <https://dx.doi.org/10.1021/jacs.0c09982>

Read Online

ACCESS |

Metrics & More

Article Recommendations

Supporting Information

**ABSTRACT:** A single molecular rhodium catalyst system ( $\text{PC2-Cp}^{\#}\text{Rh}^{\text{III}}$ ) bearing two functional domains for both photosensitization and C–H carbometalation was designed to enable an intramolecular redox process. The hypothesized charge-transfer species ( $\text{PC2}^{\bullet-}\text{-Cp}^{\#}\text{Rh}^{\text{IV}}$ ) was characterized by spectroscopic and electrochemical analyses. This photoinduced internal oxidation allows a facile access to the triplet state of the key post-transmetalation intermediate that readily undergoes C–C bond-forming reductive elimination with a lower activation barrier than in its singlet state, thus enabling catalytic C–H arylation and methylation processes.

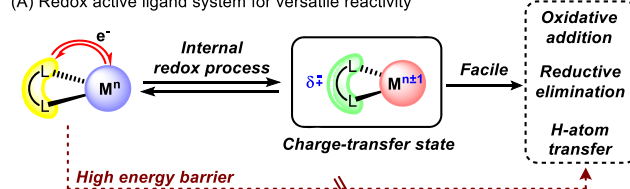
Cooperative ligand participation in transition metal catalysis has significantly expanded the scope of accessible chemical transformations either by modulating electron configuration of the metal center or via ligand–substrate interactions.<sup>1</sup> In the former case, redox noninnocent ligands, serving as an electron reservoir, are known to confer versatile catalytic reactivity by tuning the metal oxidation state.<sup>2</sup> This internal redox process often enables key elementary steps to operate readily, such as oxidative addition,<sup>3</sup> reductive elimination,<sup>4</sup> or hydrogen atom transfer,<sup>5</sup> which would be otherwise challenging (Scheme 1A). Oxidative induction of the reductive elimination process, in particular, has been of great interest as it constitutes a product-releasing step, which is often rate-limiting in a catalytic cycle.<sup>6,7</sup> This mechanistic consideration has been more pronounced for the first row metal complexes where the frontier orbitals of certain ligands are in similar levels to those of metals.<sup>8,9</sup>

In this context, light-induced metal-to-ligand charge transfer (MLCT) has emerged as a powerful tool to access higher oxidation states of the metal center in catalytic reactions (Scheme 1B, up). Recent studies demonstrated that, in addition to the more conventional outer-sphere electron transfer in photoredox catalysis,<sup>10</sup> oxidation of the metallic core via MLCT enables a targeted elementary step such as reductive elimination<sup>11</sup> or ligand transfer.<sup>12</sup> An alternative way for intramolecular modulation of the metal oxidation state was envisioned to covalently ligate a redox-active photosensitizer domain to the catalyst core (Scheme 1B, down).<sup>13</sup> In this system, upon irradiation, the excited photosensitizer moiety induces an internal redox process through the intramolecular quenching.<sup>14</sup> While these charge-transfer (CT) catalyst systems have been elegantly utilized in proton/hydride transfer and  $\text{CO}_2$  reduction processes, their application toward organic synthesis is still underdeveloped.<sup>15</sup> To our best knowledge, for example, catalytic C–H functionalization through CT-induced oxidative coupling has not been reported.

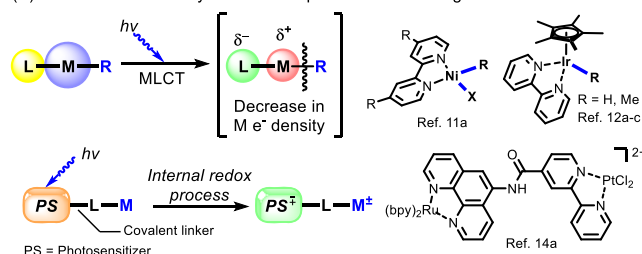
In this study, we disclose for the first time a single molecular, bimodular rhodium photocatalyst system for C–H arylation and

## Scheme 1. Facilitation of Transition Metal Catalysis with Redox-Active Ligand System

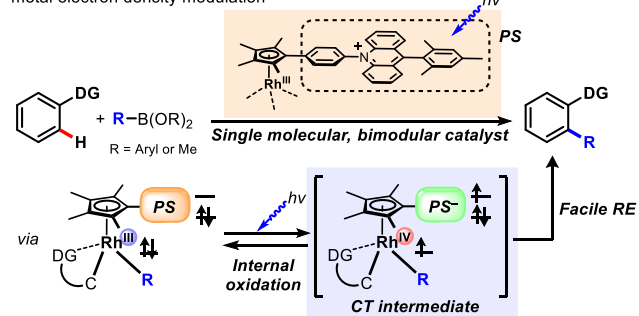
(A) Redox active ligand system for versatile reactivity



(B) Metal electron density variation via photo-induced charge transfer



(C) This work: Catalytic C–H functionalizations through charge transfer (CT)-induced metal electron density modulation



Received: September 18, 2020

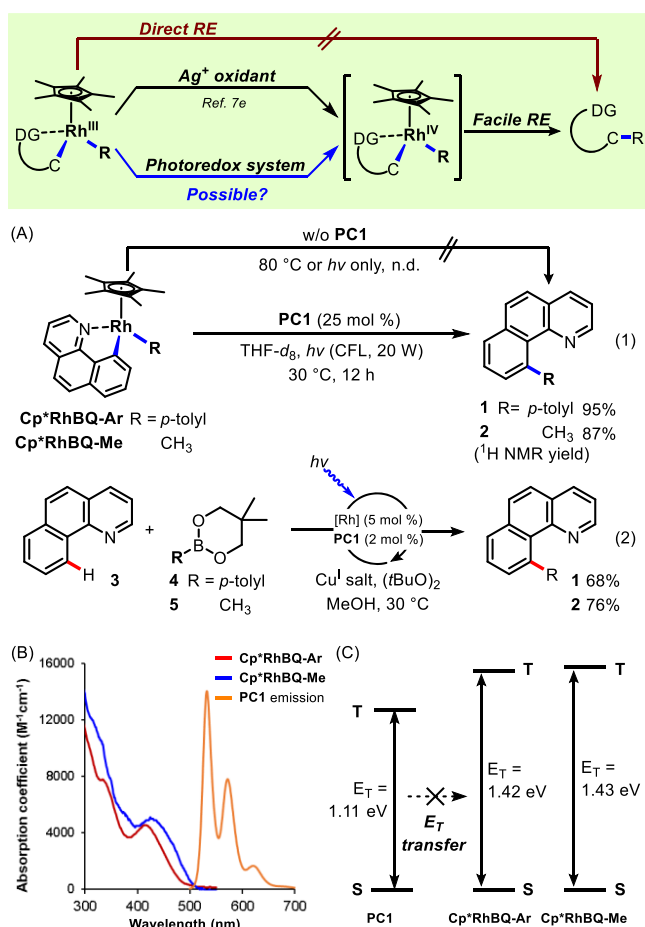


**Figure 1.** (A) Photocatalytic C–C bond forming RE from rhodacycle intermediates and its application to the catalytic C–H functionalizations. For reaction conditions, see the Supporting Information. (B) Absorption spectrum of Cp\*RhBQ-Ar and Cp\*RhBQ-Me, depicted with the emission spectrum of PC1. (C) Comparison of triplet energy of PC1 and the rhodacycle species. S, singlet state; T, triplet state.

methylation via photoinduced oxidative coupling (Scheme 1C). The working mode of the synthesized dual-functioning conjugate catalysts was verified by spectroscopic and electrochemical analysis. The formation of high-valent charge-transfer species was found to allow for the CT-induced C–C bond-forming reductive elimination from the key post-transmetalation intermediate by reducing the RE energy barrier.

On the basis of our previous result that C–C bond-forming reductive elimination from a transmetalated intermediate can be permitted by the external chemical oxidants,<sup>16a,7d,e,16b</sup> we first questioned whether the same strategy would also be operative under photoredox conditions (Figure 1A). In the presence of *N,N'*-bis(2,6-diisopropylphenyl)perylene diimide as a photocatalyst (PC1), compact fluorescent lamp (CFL)-irradiation on each solution of isolated rhodacycle species Cp\*RhBQ-Ar and Cp\*RhBQ-Me<sup>7e</sup> afforded reductive elimination products 1 and 2 in 95% and 87% yield, respectively (Figure 1, eq 1). In stark contrast, no product was formed under thermal (80 °C) or irradiation conditions in the absence of PC1, suggesting that the process is mediated by the excited photocatalyst species. We were pleased to see that this PC1 photoredox system was also operative in the Cp\*Rh-catalyzed sp<sup>2</sup> C–H arylation and methylation (Figure 1, eq 2). For instance, benzo[*h*]quinoline 3 was readily coupled with aryl and methyl boronic ester providing C-10 arylation and methylation products 1 and 2, respectively, using Cu<sup>I</sup> transmetalation agent and (*t*BuO)<sub>2</sub> as a mild terminal oxidant.

It should be noted that the fluorescence emission of PC1 did not overlap with the absorption bands of the rhodacycle Cp\*RhBQ-Ar and Cp\*RhBQ-Me (Figure 1B), thereby ruling out a dipole–dipole energy transfer mechanism for the above RE. The triplet energy of PC1 (1.11 eV) was calculated to be significantly lower than that of Cp\*RhBQ-Ar and Cp\*RhBQ-Me (1.42 and 1.43 eV, respectively), suggesting that the RE process is induced by a photocatalytic oxidation, rather than the triplet sensitization of the intermediates (Figure 1C). Indeed, the RE energy barrier from Cp\*RhBQ-Ar and Cp\*RhBQ-Me was calculated to decrease substantially from 26.7 and 28.5 kcal/mol to 6.8 and 8.6 kcal/mol, respectively, upon the single electron oxidation of the rhodium metal center, being consistent

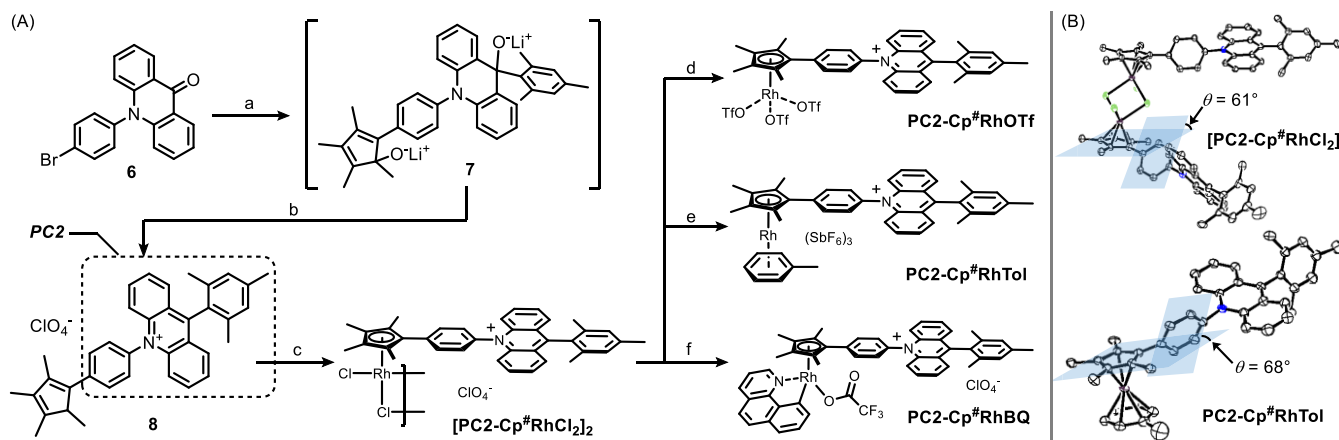


**Figure 2.** (A) Preparation of a series of Rh metallophotocatalyst bearing a mesityl acridinium (PC2) photosensitizer domain. (a) Mesityl lithium (2.0 equiv), TMEDA, Et<sub>2</sub>O, –30 to 25 °C, 26 h, then *n*BuLi (1.2 equiv), –30 to 25 °C, 3 h, then 2,3,4,5-tetramethyl-2-cyclopentenone (4.0 equiv), 25 °C, 22 h; (b) Na<sub>2</sub>CO<sub>3</sub>, H<sub>2</sub>O, EtOAc then H<sub>2</sub>O, HClO<sub>4</sub>, CH<sub>2</sub>Cl<sub>2</sub>, 25 °C, 1 h, 60% in two steps; (c) RhCl<sub>3</sub>·*x*H<sub>2</sub>O (1.0 equiv Rh), *i*PrOH, 90 °C, 14 h, 89%; (d) AgOTf (6.0 equiv), CH<sub>2</sub>Cl<sub>2</sub>, 25 °C, 14 h, 71%; (e) CH<sub>3</sub>C<sub>6</sub>H<sub>5</sub>, CH<sub>3</sub>NO<sub>2</sub>, AgSbF<sub>6</sub> (6.0 equiv), 25 °C, 14 h, 54%; (f) 3, Ag<sub>2</sub>O·CCF<sub>3</sub>, Li<sub>2</sub>CO<sub>3</sub>, CH<sub>2</sub>Cl<sub>2</sub>, 25 °C, 21 h then 40 °C, 4 h, 65%. (B) Single crystal X-ray diffraction structure of [PC2-Cp\*RhCl<sub>2</sub>]<sub>2</sub> and PC2-Cp\*RhTol. 10% thermal ellipsoids for both structures. Hydrogen atoms were omitted for clarity.

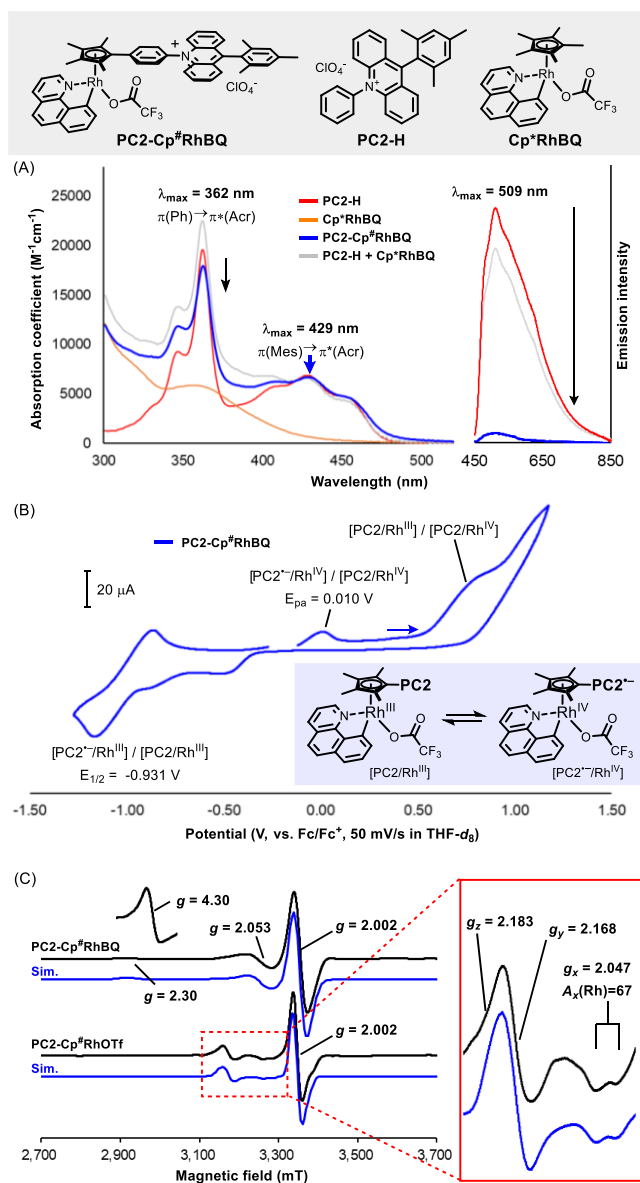
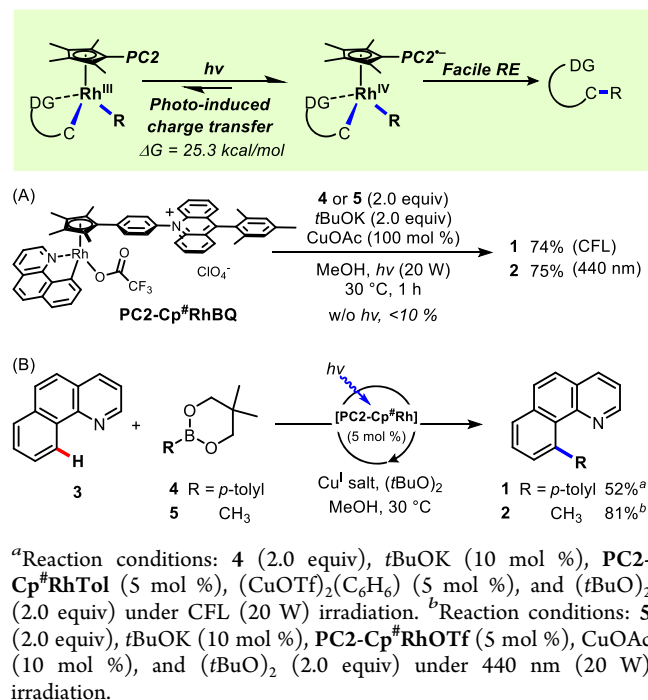


**Figure 3.** (A) UV-vis absorption (left) and fluorescence emission (right) spectrum of PC2-Cp<sup>#</sup>RhBQ, represented with that of control species. 440 nm wavelength was used for the excitation for the emission spectra. (B) Cyclic voltammogram of PC2-Cp<sup>#</sup>RhBQ in THF-*d*<sub>8</sub> at 50 mV/s. (C) Experimental (black) X-band EPR spectrum of PC2-Cp<sup>#</sup>RhBQ and PC2-Cp<sup>#</sup>RhOTf in CH<sub>2</sub>Cl<sub>2</sub> at 100 K and simulated (blue) EPR spectrum for each case.

with the mild reaction conditions (see the Supporting Information for details).<sup>7d,e</sup>

Encouraged by the above initial results that the product-delivering oxidatively induced reductive elimination is enabled by the external photoredox catalyst, we were challenged to design a bimodular rhodium photocatalyst system bearing two functional domains in a single molecule, thus capable of both photosensitization and C-H functionalization. In this context, we envisioned to covalently link a photosensitizer to a synthetically tunable cyclopentadienyl ligand to induce an *internal oxidation* of the metal center upon irradiation, thus eventually permitting the oxidatively induced RE process. To this end, we readily synthesized a ligand **8** bearing a 10-mesityl-9-phenylacridinium (PC2) moiety linked to the cyclopenta-

## Scheme 2. Light-Induced RE Process from PC2-Cp<sup>#</sup>Rh Catalyst System and Its Application to the Catalytic C-H Functionalizations



<sup>a</sup>Reaction conditions: **4** (2.0 equiv), *t*BuOK (10 mol %), PC2-Cp<sup>#</sup>RhTol (5 mol %), (CuOTf)<sub>2</sub>(C<sub>6</sub>H<sub>6</sub>) (5 mol %), and (*t*BuO)<sub>2</sub> (2.0 equiv) under CFL (20 W) irradiation. <sup>b</sup>Reaction conditions: **5** (2.0 equiv), *t*BuOK (10 mol %), PC2-Cp<sup>#</sup>RhOTf (5 mol %), CuOAc (10 mol %), and (*t*BuO)<sub>2</sub> (2.0 equiv) under 440 nm (20 W) irradiation.

dienyl ring, where the phenylene linker was expected to bridge the two conjugate systems, starting from a commercially available acridone derivative **6** (Figure 2A). Complexation of this ligand to a Rh precursor afforded a dimeric rhodium species [PC2-Cp<sup>#</sup>RhCl<sub>2</sub>]<sub>2</sub> (Cp<sup>#</sup> = -C<sub>5</sub>Me<sub>4</sub>) in high yield, and its structure was confirmed by a single crystal X-ray diffraction analysis to show that the phenyl group is staggered (61°) with respect to the cyclopentadienyl ring (Figure 2B). The dimeric precursor [PC2-Cp<sup>#</sup>RhCl<sub>2</sub>]<sub>2</sub> was then treated with silver salts to obtain monomeric rhodium complexes PC2-Cp<sup>#</sup>RhOTf and PC2-Cp<sup>#</sup>RhTol, and the X-ray crystallographic structure of the latter was determined, displaying  $\eta^6$ -coordination mode of the toluene ligand on the rhodium center.<sup>17</sup>

A rhodacycle complex PC2-Cp<sup>#</sup>RhBQ was also prepared by a facile carbometalation of benzo[*h*]quinoline **3** to [PC2-Cp<sup>#</sup>RhCl<sub>2</sub>]<sub>2</sub>, and the *ipso* carbon was characterized by observing a doublet signal in <sup>13</sup>C NMR spectrum ( $\delta$  175.0 ppm, <sup>2</sup>J<sub>Rh-C</sub> = 34.1 Hz in CD<sub>2</sub>Cl<sub>2</sub>). Additional spectroscopic and electrochemical analyses on PC2-Cp<sup>#</sup>RhBQ were performed in comparison with the photosensitizer segment (PC2-H) as well as the parent rhodacycle Cp<sup>#</sup>RhBQ (Figure 3A). An absorbance at 362 nm, which corresponds to the phenyl ( $\pi$ ) to acridinium ( $\pi^*$ ) transition in PC2-H, was decreased in the PC2-Cp<sup>#</sup>RhBQ conjugate, while that at 429 nm remained unchanged, which was ascribed to the mesityl ( $\pi$ ) to acridinium ( $\pi^*$ ) transition. In addition, phosphorescence at 509 nm of PC2-H was almost completely suppressed in PC2-Cp<sup>#</sup>RhBQ, implying that an intramolecular quenching takes place dominantly for the relaxation.<sup>14a</sup>

On the other hand, the cyclic voltammogram of PC2-Cp<sup>#</sup>RhBQ showed one unexpected irreversible oxidation peak at  $E_{\text{pa}} = 0.010$  V (50 mV/s, vs Fc/Fc<sup>+</sup>) in addition to the anticipated signals assignable to photocatalyst redox pair ([PC2<sup>-</sup>/PC2]) and Rh<sup>III</sup>/Rh<sup>IV</sup> oxidation, even without

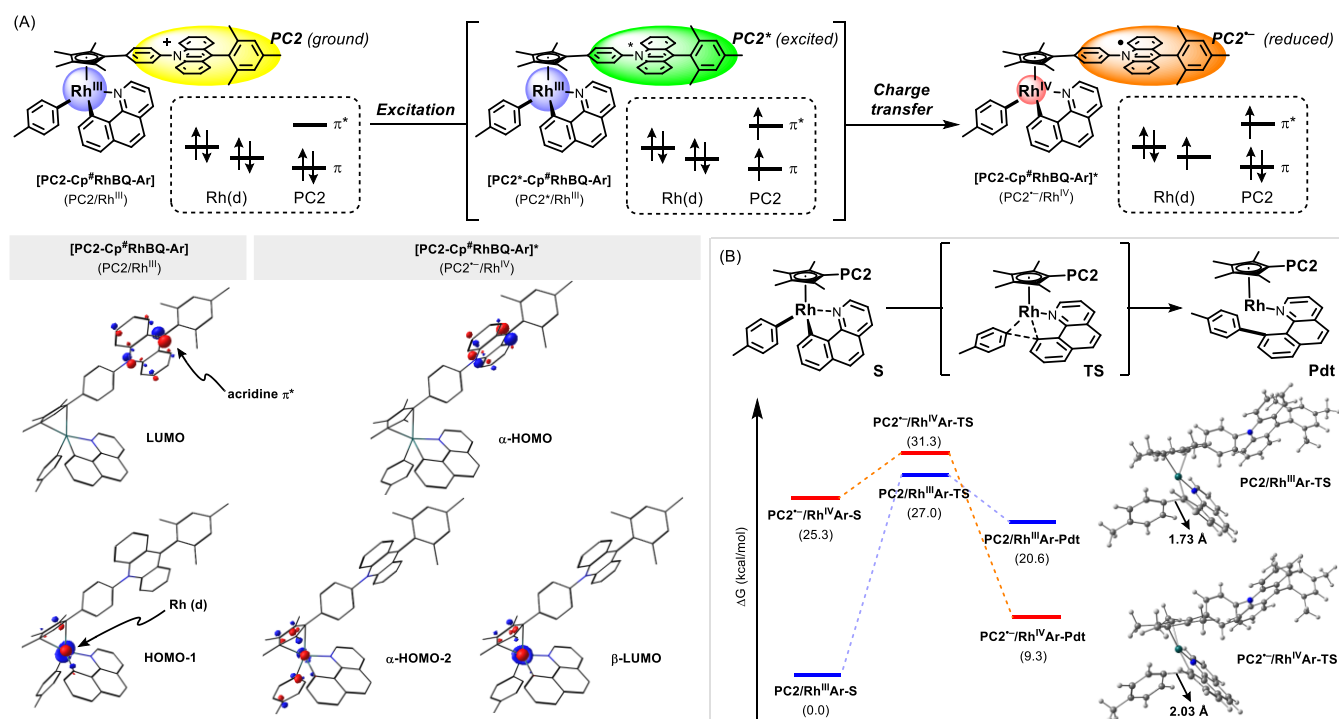


**Figure 4.** DFT calculation studies on the hypothetical  $\text{PC2-Cp}^\# \text{RhBQ-Ar}$  species.  $\epsilon = 7.4257$  for tetrahydrofuran. (A) Schematic diagram for the light-induced internal charge transfer process and Kohn–Sham diagram of the frontier orbitals for  $\text{PC2-Cp}^\# \text{RhBQ-Ar}$  in singlet and triplet ground state. Isovalue = 0.1. (B) The activation barriers for reductive elimination from singlet (blue) and triplet (red) states of  $\text{PC2-Cp}^\# \text{RhBQ-Ar}$ , depicted with the transition state geometry. For the methyl counterpart, see the [Supporting Information](#).

irradiation (Figure 3B). The signal at  $E_{\text{pa}} = 0.010$  V was assigned to the oxidation arising from the metal-to-photosensitizer charge-transfer state,  $\text{PC2}^{\bullet-}/\text{Rh}^{\text{IV}}$ , which is assumed to be present in equilibrium with the ground state,  $\text{PC2}/\text{Rh}^{\text{III}}$ . Indeed, the X-band EPR spectrum of  $\text{PC2-Cp}^\# \text{RhBQ}$  displayed signals corresponding to organic radical ( $g = 2.002$ ) and transition metal ion ( $g = 2.053$  and  $2.30$ ) as well as a high-spin unpaired electron ( $g = 4.30$ , Figure 3C). The line broadening of the organic radical signal can be ascribed to the hyperfine coupling by the acridine nitrogen, where the  $\alpha$ -HOMO of the triplet rhodacycle species is distributed (vide infra). Furthermore, the hyperfine coupling by the Rh metal center was detected in the metal-centered rhombic resonance of  $\text{PC2-Cp}^\# \text{RhOTf}$  ( $g_x = 2.047$ ), indicating the transient formation of a high-valent  $\text{Rh}^{\text{IV}}$  species by the photosensitizer moiety (PC2).

Having found that the photosensitizer domain can easily access the rhodium valence electrons, we envisaged that the  $\text{PC2-Cp}^\# \text{Rh}$ -mediated C–C bond-forming RE process could be promoted by the action of light-excited chromophore domain ( $\text{PC2}^*$ ) through an internal oxidation of the metal center. Indeed, when a solution of  $\text{PC2-Cp}^\# \text{RhBQ}$  was irradiated in the presence of aryl- or methyl borate (4 and 5) and Cu(I) transmetalation agent, the desired reductive elimination products (1 and 2, respectively) were obtained in good yields (Scheme 2A). However, reactions in dark afforded products in less than 10% yields, again suggesting that this process is facilitated by the light-induced internal charge transfer. Moreover, catalytic C–H functionalization by using  $\text{PC2-Cp}^\# \text{Rh}$  catalyst system was also successfully performed under irradiation conditions (Scheme 2B).

Finally, DFT calculations on the postulated intermediate  $\text{PC2-Cp}^\# \text{RhBQ-Ar}$  were carried out for better understanding of the light-induced RE process. The frontier molecular orbital

diagram for the singlet ground state represents metal-centered occupied frontier orbitals (HOMO and HOMO–1) and acridine ( $\pi^*$ )-centered LUMO (Figure 4A). On the other hand, in the triplet ground state ( $[\text{PC2-Cp}^\# \text{RhBQ-Ar}]^*$ ), while the  $\alpha$ -HOMO is located on the acridine  $\pi^*$ , the  $\beta$ -LUMO is mainly composed of nonbonding metal d orbitals which dominantly comprise metal-centered HOMO–1 of the singlet state. Furthermore, the RE energy barrier of the postulated  $\text{PC2-Cp}^\# \text{RhBQ-Ar}$  intermediate decreases from 27.0 to 6.0 kcal/mol upon the charge transfer, implying that the triplet excitation in the photosensitizer domain will result in an internal oxidation to form a transient  $\text{Rh}^{\text{IV}}$  species, from which the C–C forming RE process readily takes place (Figure 4B). A similar tendency was also observed for the methyl analogue  $\text{PC2-Cp}^\# \text{RhBQ-Me}$ , where the activation energy of RE was also substantially reduced from 30.0 to 11.1 kcal/mol upon the charge transfer (see the [Supporting Information](#) for details).

In conclusion, a single molecular rhodium catalyst system bearing two functional domains for photosensitization and C–H carbometalation was successfully developed for the first time. It was shown that the excited photosensitizer moiety generates a transient high-valent  $\text{Rh}^{\text{IV}}$  intermediate through an internal oxidation, thus facilitating the key C–C bond-forming reductive elimination process in the oxidative C–H arylation and methylation reactions.

## ■ ASSOCIATED CONTENT

### Supporting Information

The Supporting Information is available free of charge at <https://pubs.acs.org/doi/10.1021/jacs.0c09982>.

Experimental procedures; characterization data; spectra for all new compounds; Cartesian coordinates of all computed structures (PDF)

Crystallographic data for  $\text{Cp}^*\text{RhBQ-Ar}$  (CIF)  
Crystallographic data for  $[\text{PC2-Cp}^*\text{RhCl}_2]_2$  (CIF)  
Crystallographic data for  $\text{PC2-Cp}^*\text{RhTol}$  (CIF)

## AUTHOR INFORMATION

### Corresponding Author

**Sukbok Chang** – Center for Catalytic Hydrocarbon Functionalization, Institute for Basic Science (IBS), Daejeon 34141, South Korea; Department of Chemistry, Korea Advanced Institute of Science and Technology (KAIST), Daejeon 34141, South Korea; [orcid.org/0000-0001-9069-0946](https://orcid.org/0000-0001-9069-0946); Email: [sbchang@kaist.ac.kr](mailto:sbchang@kaist.ac.kr)

### Authors

**Jinwoo Kim** – Department of Chemistry, Korea Advanced Institute of Science and Technology (KAIST), Daejeon 34141, South Korea; Center for Catalytic Hydrocarbon Functionalization, Institute for Basic Science (IBS), Daejeon 34141, South Korea

**Dongwook Kim** – Center for Catalytic Hydrocarbon Functionalization, Institute for Basic Science (IBS), Daejeon 34141, South Korea; [orcid.org/0000-0003-4432-371X](https://orcid.org/0000-0003-4432-371X)

Complete contact information is available at:  
<https://pubs.acs.org/10.1021/jacs.0c09982>

### Notes

The authors declare no competing financial interest.

## ACKNOWLEDGMENTS

This paper is dedicated to Professor Pierre Dixneuf for his outstanding contributions to organometallic chemistry and catalysis. This research was supported by the Institute for Basic Science (IBS-R010-D1) in Republic of Korea. Single crystal X-ray diffraction experiments with synchrotron radiation were performed at the BL2D-SMC in Pohang Accelerator Laboratory.

## REFERENCES

- (1) (a) *Ligand Design in Metal Chemistry: Reactivity and Catalysis*; Stradiotto, M., Lundgren, R. J., Eds.; John Wiley & Sons, Ltd., 2016. (b) Grützmacher, H. Cooperating Ligands in Catalysis. *Angew. Chem., Int. Ed.* **2008**, *47*, 1814–1818. (c) Khusnutdinova, J. R.; Milstein, D. Metal–Ligand Cooperation. *Angew. Chem., Int. Ed.* **2015**, *54*, 12236–12273.
- (2) (a) Lyaskovskyy, V.; de Bruin, B. Redox Non-Innocent Ligands: Versatile New Tools to Control Catalytic Reactions. *ACS Catal.* **2012**, *2*, 270–279. (b) van der Vlugt, J. I. Radical-Type Reactivity and Catalysis by Single-Electron Transfer to or from Redox-Active Ligands. *Chem. - Eur. J.* **2019**, *25*, 2651–2662.
- (3) (a) Blackmore, K. J.; Ziller, J. W.; Heyduk, A. F. Oxidative Addition to a Zirconium(IV) Redox-Active Ligand Complex. *Inorg. Chem.* **2005**, *44*, 5559–5561. (b) Haneline, M. R.; Heyduk, A. F. C–C Bond-Forming Reductive Elimination from a Zirconium(IV) Redox-Active Ligand Complex. *J. Am. Chem. Soc.* **2006**, *128*, 8410–8411. (c) Smith, A. L.; Hardcastle, K. I.; Soper, J. D. Redox-Active Ligand-Mediated Oxidative Addition and Reductive Elimination at Square Planar Cobalt(III): Multielectron Reactions for Cross-Coupling. *J. Am. Chem. Soc.* **2010**, *132*, 14358–14360. (d) Arevalo, R.; Chirik, P. J. Enabling Two-Electron Pathways with Iron and Cobalt: From Ligand Design to Catalytic Applications. *J. Am. Chem. Soc.* **2019**, *141*, 9106–9123.
- (4) (a) Bart, S. C.; Chlopek, K.; Bill, E.; Bouwkamp, M. W.; Lobkovsky, E.; Neese, F.; Wieghardt, K.; Chirik, P. J. Electronic Structure of Bis(imino)pyridine Iron Dichloride, Monochloride, and Neutral Ligand Complexes: A Combined Structural, Spectroscopic, and Computational Study. *J. Am. Chem. Soc.* **2006**, *128*, 13901–13912. (b) Jones, G. D.; Martin, J. L.; McFarland, C.; Allen, O. R.; Hall, R. E.; Haley, A. D.; Brandon, R. J.; Kononova, T.; Desrochers, P. J.; Pulay, P.; Vacic, D. A. Ligand Redox Effects in the Synthesis, Electronic Structure, and Reactivity of an Alkyl–Alkyl Cross-Coupling Catalyst. *J. Am. Chem. Soc.* **2006**, *128*, 13175–13183.
- (5) (a) Salanouve, E.; Bouzemale, G.; Blanchard, S.; Derat, E.; Desage-El Murr, M.; Fensterbank, L. Tandem C–H Activation/Arylation Catalyzed by Low-Valent Iron Complexes with Bisiminopyridine Ligands. *Chem. - Eur. J.* **2014**, *20*, 4754–4761. (b) Morton, C. M.; Zhu, Q.; Ripberger, H.; Troian-Gautier, L.; Toa, Z. S. D.; Knowles, R. R.; Alexanian, E. J. C–H Alkylation via Multisite-Proton-Coupled Electron Transfer of an Aliphatic C–H Bond. *J. Am. Chem. Soc.* **2019**, *141*, 13253–13260.
- (6) Poli, R. Open shell organometallics as a bridge between Werner-type and low-valent organometallic complexes. The effect of the spin state on the stability, reactivity, and structure. *Chem. Rev.* **1996**, *96*, 2135–2204.
- (7) (a) Li, L.; Brennessel, W. W.; Jones, W. D. An Efficient Low-Temperature Route to Polycyclic Isoquinoline Salt Synthesis via C–H Activation with  $[\text{Cp}^*\text{MCl}_2]_2$  (M = Rh, Ir). *J. Am. Chem. Soc.* **2008**, *130*, 12414–12419. (b) Wolf, W. J.; Winston, M. S.; Toste, F. D. Exceptionally fast carbon–carbon bond reductive elimination from gold(III). *Nat. Chem.* **2014**, *6*, 159–164. (c) Yang, Q.-L.; Li, Y.-Q.; Ma, C.; Fang, P.; Zhang, X.-J.; Mei, T.-S. Palladium-Catalyzed  $\text{C}(\text{sp}^3)$ –H Oxygenation via Electrochemical Oxidation. *J. Am. Chem. Soc.* **2017**, *139*, 3293–3298. (d) Shin, K.; Park, Y.; Baik, M. H.; Chang, S. Iridium-catalysed arylation of C–H bonds enabled by oxidatively induced reductive elimination. *Nat. Chem.* **2018**, *10*, 218–224. (e) Kim, J.; Shin, K.; Jin, S.; Kim, D.; Chang, S. Oxidatively Induced Reductive Elimination: Exploring the Scope and Catalyst Systems with Ir, Rh, and Ru Complexes. *J. Am. Chem. Soc.* **2019**, *141*, 4137–4146. (f) Roberts, C. C.; Chong, E.; Kampf, J. W.; Canty, A. J.; Ariafard, A.; Sanford, M. S. Nickel(II/IV) Manifold Enables Room-Temperature  $\text{C}(\text{sp}^3)$ –H Functionalization. *J. Am. Chem. Soc.* **2019**, *141*, 19513–19520.
- (8) (a) Gulliver, D. J.; Levason, W. The chemistry of ruthenium, osmium, rhodium, iridium, palladium and platinum in the higher oxidation states. *Coord. Chem. Rev.* **1982**, *46*, 1–127. (b) Storr, T.; Verma, P.; Pratt, R. C.; Wasinger, E. C.; Shimazaki, Y.; Stack, T. D. P. Defining the Electronic and Geometric Structure of One-Electron Oxidized Copper–Bis-phenoxide Complexes. *J. Am. Chem. Soc.* **2008**, *130*, 15448–15459. (c) Pierpont, C. G. Ligand Redox Activity and Mixed Valency in First-Row Transition-Metal Complexes Containing Tetrachlorocatecholate and Radical Tetrachlorosemiquinonate Ligands. *Inorg. Chem.* **2011**, *50*, 9766–9772.
- (9) (a) Kotani, H.; Sugiyama, T.; Ishizuka, T.; Shiota, Y.; Yoshizawa, K.; Kojima, T. Redox-Noninnocent Behavior of Tris(2-pyridylmethyl)-amine Bound to a Lewis Acidic Rh(III) Ion Induced by C–H Deprotonation. *J. Am. Chem. Soc.* **2015**, *137*, 11222–11225. (b) Fujita, D.; Sugimoto, H.; Morimoto, Y.; Itoh, S. Noninnocent Ligand in Rhodium(III)-Complex-Catalyzed C–H Bond Amination with Tosyl Azide. *Inorg. Chem.* **2018**, *57*, 9738–9747.
- (10) (a) Tucker, J. W.; Stephenson, C. R. Shining light on photoredox catalysis: theory and synthetic applications. *J. Org. Chem.* **2012**, *77*, 1617–1622. (b) Prier, C. K.; Rankic, D. A.; MacMillan, D. W. Visible light photoredox catalysis with transition metal complexes: applications in organic synthesis. *Chem. Rev.* **2013**, *113*, 5322–5363.
- (11) (a) Welin, E. R.; Le, C.; Arias-Rotondo, D. M.; McCusker, J. K.; MacMillan, D. W. C. Photosensitized, energy transfer-mediated organometallic catalysis through electronically excited nickel(II). *Science* **2017**, *355*, 380–385. (b) Ma, P.; Wang, S.; Chen, H. Reactivity of Transition-Metal Complexes in Excited States: C–O Bond Coupling Reductive Elimination of a Ni(II) Complex Is Elicited by the Metal-to-Ligand Charge Transfer State. *ACS Catal.* **2020**, *10*, 1–6.
- (12) (a) Ziesel, R. Photocatalysis. Mechanistic studies of homogeneous photochemical water gas shift reaction catalyzed under mild conditions by novel cationic iridium(III) complexes. *J. Am. Chem. Soc.* **1993**, *115*, 118–127. (b) Suenobu, T.; Guldi, D. M.; Ogo, S.;

Fukuzumi, S. Excited-State Deprotonation and H/D Exchange of an Iridium Hydride Complex. *Angew. Chem., Int. Ed.* **2003**, *42*, 5492–5495. (c) Pitman, C. L.; Miller, A. J. M. Photochemical Production of Ethane from an Iridium Methyl Complex. *Organometallics* **2017**, *36*, 1906–1914.

(13) (a) Schulz, M.; Karnahl, M.; Schwalbe, M.; Vos, J. G. The role of the bridging ligand in photocatalytic supramolecular assemblies for the reduction of protons and carbon dioxide. *Coord. Chem. Rev.* **2012**, *256*, 1682–1705. (b) Stoll, T.; Castillo, C. E.; Kayanuma, M.; Sandroni, M.; Daniel, C.; Odobel, F.; Fortage, J.; Collomb, M. N. Photo-induced redox catalysis for proton reduction to hydrogen with homogeneous molecular systems using rhodium-based catalysts. *Coord. Chem. Rev.* **2015**, *304*, 20–37.

(14) (a) Ozawa, H.; Haga, M.-a.; Sakai, K. A Photo-Hydrogen-Evolving Molecular Device Driving Visible-Light-Induced EDTA-Reduction of Water into Molecular Hydrogen. *J. Am. Chem. Soc.* **2006**, *128*, 4926–4927. (b) Lentz, C.; Schott, O.; Auvray, T.; Hanan, G.; Elias, B. Photocatalytic Hydrogen Production Using a Red-Absorbing Ir(III)–Co(III) Dyad. *Inorg. Chem.* **2017**, *56*, 10875–10881. (c) Manbeck, G. F.; Fujita, E.; Brewer, K. J. Tetra- and Heptametallic Ru(II),Rh(III) Supramolecular Hydrogen Production Photocatalysts. *J. Am. Chem. Soc.* **2017**, *139*, 7843–7854.

(15) (a) Böhm, A.; Bach, T. Synthesis of Supramolecular Iridium Catalysts and Their Use in Enantioselective Visible-Light-Induced Reactions. *Synlett* **2016**, *27*, 1056–1060. (b) Gandeepan, P.; Koeller, J.; Korvorapun, K.; Mohr, J.; Ackermann, L. Visible-Light-Enabled Ruthenium-Catalyzed meta-C–H Alkylation at Room Temperature. *Angew. Chem., Int. Ed.* **2019**, *58*, 9820–9825. (c) Sagadevan, A.; Greaney, M. F. meta-Selective C–H Activation of Arenes at Room Temperature Using Visible Light: Dual-Function Ruthenium Catalysis. *Angew. Chem., Int. Ed.* **2019**, *58*, 9826–9830. (d) Thongpaen, J.; Manguin, R.; Dorcet, V.; Vives, T.; Duhayon, C.; Mauduit, M.; Baslé, O. Visible Light Induced Rhodium(I)-Catalyzed C–H Borylation. *Angew. Chem., Int. Ed.* **2019**, *58*, 15244–15248. (e) Gao, Y.; Yang, C.; Bai, S.; Liu, X.; Wu, Q.; Wang, J.; Jiang, C.; Qi, X. Visible-Light-Induced Nickel-Catalyzed Cross-Coupling with Alkylzirconocenes from Unactivated Alkenes. *Chem.* **2020**, *6*, 675–688. (f) Korvorapun, K.; Struwe, J.; Kuniyil, R.; Zangarelli, A.; Casnati, A.; Waeterschoot, M.; Ackermann, L. Photo-Induced Ruthenium-Catalyzed C–H Arylations at Ambient Temperature. *Angew. Chem., Int. Ed.* **2020**, *59*, 18103–18109. (g) Sagadevan, A.; Charitou, A.; Wang, F.; Ivanova, M.; Vuagnat, M.; Greaney, M. F. Ortho C–H arylation of arenes at room temperature using visible light ruthenium C–H activation. *Chem. Sci.* **2020**, *11*, 4439–4443.

(16) (a) Shin, K.; Park, S.-W.; Chang, S. Cp\*Ir(III)-Catalyzed Mild and Broad C–H Arylation of Arenes and Alkenes with Aryldiazonium Salts Leading to the External Oxidant-Free Approach. *J. Am. Chem. Soc.* **2015**, *137*, 8584–8592. (b) Xie, W.; Heo, J.; Kim, D.; Chang, S. Copper-Catalyzed Direct C–H Alkylation of Polyfluoroarenes by Using Hydrocarbons as an Alkylating Source. *J. Am. Chem. Soc.* **2020**, *142*, 7487–7496.

(17) Maekawa, M.; Hashimoto, N.; Kuroda-Sowa, T.; Suenaga, Y.; Munakata, M. Crystal Structure of  $\eta^5$ -Pentamethylcyclopentadienyl- $\eta^6$ -toluene Rhodium Tetrafluoroborate,  $[\text{Rh}(\text{Cp}^*)(\eta^6\text{-C}_6\text{H}_5\text{Me})](\text{BF}_4)_2$  ( $\text{Cp}^* = \eta^5\text{-C}_5\text{Me}_5$ ). *Anal. Sci.* **2001**, *17*, 1361–1362.